Influence of Calcination Parameters on Alumina Quality in Gas Suspension Calciner

Bharathesh Kumar[1], Nireesh Budumuru[1], Swapnil Ghatage[2], Chandrakala Kari[3], Vilas Tathavadkar[4], Keshav Karn[5], Neelamani Srivatsav[5], Himanshu Ranjan[6] and Paul Gupta[7]
1. Scientist
2. Senior scientist
3. Lead scientist
4. President and Function Head, Metals & Mining
Aditya Birla Science & Technology Company, Navi Mumbai, India.
5. Assistant General Manager
6. General Manager
Hindalco Industries, Renukoot, India
7. Assistant Vice President
Utkal Alumina International, Rayagada, India
Corresponding author: chandrakala.kari@adityabirla.com
https://doi.org/10.71659/icsoba2024-aa029

Abstract

Improving the alumina calcination process with the objectives to reduce specific fuel energy consumption and enhance product quality has been the driver of recent technological advancements. Alumina quality in terms of parameters such as LOI, surface area and phase composition impact the efficiency of downstream smelting process. Gamma alumina is often considered the most desirable phase from a pure dissolution perspective; the operating parameters of the calciner has profound impact on the phase transformation reactions and final phase composition. In this work, calciner operation is optimized using computational fluid dynamics (CFD). The optimum thermal profile is obtained by simulating cases with various air-to-fuel ratios. Fairly good agreement has been obtained with the available temperature measurements that were recorded for model validation. The physical and phase analysis reveals that the final alumina is over-calcined with the current operational strategy. In addition, a non-uniform solid and gas flow is observed in furnace at a wide range of operating parameters. The CFD simulations indicate that for the particular calciner examined; more uniform air/solid distribution and mixing are achieved by maintaining an air to fuel ratio of approximately ~23. Onsite trials have been conducted to reduce the calciner temperature from 1140 °C to 1075 °C. The result indicated an increase of LOI and specific surface area from 0.4 to 0.7, and from 58 m^2/g to 74 m^2/g, respectively, thereby meeting the quality requirements of smelting grade alumina.

Keywords: Alumina calcination, Gas suspension calciner, Specific surface area, Combustion, CFD modeling.

1. Introduction

The metallurgical grade alumina required for smelting is predominantly produced through the Bayer process. During the process, selective dissolution and precipitation of aluminium hydroxide takes place. The precipitated aluminium hydroxide is then calcined to form polycrystalline grains of aluminium oxide. The fundamentals of the Bayer process have remained largely unchanged since its invention and will likely continue to be the primary method used to produce smelting grade of alumina in the future [1]. However, the calcination conditions dictate the many of the parameters that determine the quality of the alumina for smelting requirements.

During calcination, the aluminium hydroxide ($Al(OH)_3$) gets converted to a series of transition alumina based on the temperature and residence time. The thermal treatment leads to conversion of hydroxide to water, however certain structural hydroxyls get retained which is quantified as "Loss on Ignition (LOI)". The commonly found phases in smelting grade alumina are gamma, delta, theta and alpha [2]. From an economic perspective, many technological advancements have been made, however, the quality of alumina has received less attention. In refineries, higher attention is given on the percentage of alpha content in comparison to the rest of the transition phases as alpha is easier to quantify and monitor. In addition, it also causes adverse effects in aluminium smelting, which is explained in detail below.

The alpha phase of alumina is the final stable form of alumina with loss on ignition (LOI) content close to negligible. However, typical smelter grade alumina has an LOI near to ~1 wt %. During aluminium smelting, transition alumina is favoured for alumina dissolution in the electrolyte bath due to better dispersion. The electrolyte bath is usually maintained at temperature close to 950 ºC. When the transition alumina comes in contact with the bath, the hydroxide content (OH) reacts to form HF and immediately releases as gas causing local agitation. This helps in the rapid dispersion of the alumina which promotes dissolution. When the LOI content in alumina increase above permissible limit, the excess HF formation results in the loss of bath [3].

The low temperature calcined material such as gamma alumina possess lower funnel time (for flowability) and higher surface area in comparison with high temperature calcined alpha alumina [4]. The phases after gamma alumina, are prone to formation of lumps in the bath, hampering the dissolution rate with formation of sludge. Sludge formation is one of the major reasons for the decrease in the current efficiency and increase of the energy demand in smelting. It also affects the metal recovery and hampers the productivity of smelter [5].

Unfortunately, in refineries, there is a rare practice of measurement for intermediate phases and only alpha content is quantified. Also, the impact of various phases on smelting is less understood. Due to these reasons, the operation of calciner may get deviated from the optimal range. Maintaining and prioritizing the alumina characteristics are essential for efficient functioning of smelter. It is most important to produce desired grades of alumina, which immediately dissolve in the electrolyte bath. This has been discussed thoroughly and listed as one of the important objectives for 21st century in the Alumina Roadmap [6]. There is an ongoing debate about the ideal quality of alumina for smelting purposes. Different smelting technologies may require specific qualities of alumina. At many situations, a single smelting unit might be purchasing alumina from different refineries to support the needs of production demand. If the quality of alumina is dissimilar, then it may cause decrease in the performance and productivity of smelter.

For producing smelting grade alumina, many refineries use so called static calciners such as gas suspension, fluid flash or circulating fluidised bed calciners in favour of less energy efficient rotary kilns. These static calciners operate on the principle of fluidization. The impacts of high heating rates and residence time can be observed on the structural properties of alumina in terms of morphology and pore structure. Since these are operated with high air flowrates with high velocities, depending on the strength of gibbsite particle, the percentage of fines may increase considerably after calcination. Due to both internal recirculation as well as heat and mass transfer effects, these fine particles tend to get more calcined increasing the alpha phase [7]. Slight variation in the hydrodynamic parameters can induce uneven flow pattern inside the furnace, impacting the quality of alumina. Hence, it is crucial to study the internal flow pattern i.e. hydrodynamics along with fuel combustion. Moreover, it is important to take a holistic approach, considering both the alumina properties and how these impact the performance of the alumina when used as a feedstock in downstream smelting and dry-scrubbing applications. Therefore, in this paper, an attempt has been made to bridge the gap between the Bayer and Hall-Héroult process in terms of quality of final calcined alumina.

The characterization methods such as X-Ray Diffraction (XRD), Brunauer–Emmett–Teller (BET) and scanning electron microscopy (SEM) are used to assess the quality of alumina. Computational fluid dynamics (CFD) is a powerful tool for detailed understanding of fluid dynamics, solid-gas interactions as well as fuel combustion along with heat transfer effects. It can be used to study and optimise calciner operating parameters such as air to fuel ratio. An overview of the calcination process and detailed methodologies of analytical characterization and modelling are described in section 2. The key results and insights from BET, XRD, SEM and CFD analysis are discussed in section 3. Onsite trials are conducted based on the optimization studies and results are presented supporting the production of improved quality of alumina in calcination.

2. Technical Approach

2.1 Overview of the Calcination Process

In the present work, the studies are performed on the world's first gas suspension calciner in the alumina industry, established by FLSmidth at Hindalco Industries Ltd, Renukoot in 1986. The calciner is able to produce up to 1200 metric ton per day (TPD) of calcined alumina.

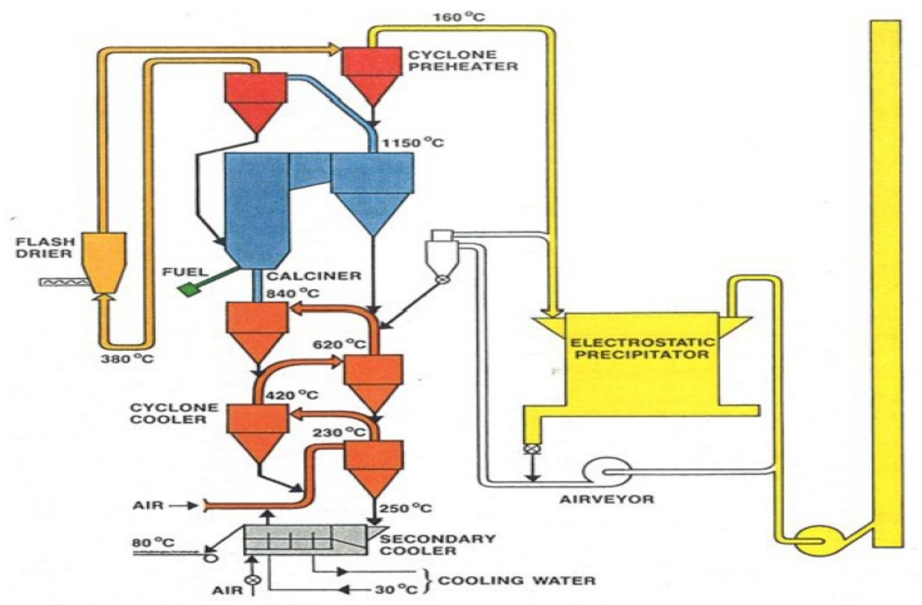

Figure 1. Process flow diagram of GSC calciner.

The process flow diagram of the gas suspension calciner (GSC) is shown in Figure 1. It is a single pass circuit with an operating pressure lower than the atmospheric pressure. An induced draft fan produces suction enough for counter current transport of solids and air. The temperature required for the calcination is achieved in the furnace and solid particles are separated in a cyclone shown in blue colour in Figure 1. The preheated air enters the furnace at the bottom from cooling cyclone. The preheated Gibbsite (or aluminium hydroxide) particles are fed through a nozzle located in the furnace. The furnace consists of 4 equally spaced burners close to the bottom for spraying the fuel i.e. Low Sulphur Heavy Stock (LSHS). The flue gas exits the separating cyclone towards the preheating section. The preheating section consists of two cyclones for material transport and heat transfer. The heat from hot calcined alumina is recovered through passing the solids over four cooling cyclones.

The calciner furnace is generally operated at a temperature of approximately 1150 °C using LSHS as fuel with calorific value ranging from 10 400 to 10 700 kcal/kg. The average specific fuel energy consumption is around 3 250 kJ/kg compared to the design value of 3 100 kJ/kg [8]. Other new generation gas suspension calciners within Hindalco are operated with a lower specific fuel energy consumption i.e. below 2 800 kJ/kg. This indicates an opportunity for the potential energy saving by operating the furnace at the optimal conditions.

2.2 Characterization

To identify the phases and their crystallinity of alumina powder, X ray diffraction study was carried out using Malvern Panalytical Empyrean DY-2482 (using CuKα X-rays). Samples were scanned n the range $5° \leq 2\theta \leq 80°$ with a step size of 0.02°. The quantification analysis was carried out using Highscore plus software (Rietveld analysis). The major characteristics such as background, zero displacement, the scale factors, the peak breadth, the unit cell parameter are considered during refinement. The quality of analysis was quantified using the weighted summation of residual of the least squares fit, R_{wp}, the statistically expected least squares fit, R_{exp}, and the goodness of fit (GoF = R_{wp} / R_{exp}). The surface area was determined using multiple-point Brunauer- Emmett-Teller (BET) method using nitrogen adsorption (Quantachrome Nova 1000e). The morphology and pore structures are characterized using scanning electron microscopy (SEM) instrument, Hitachi-S 4800.

2.3 Numerical Methodology

The numerical studies are carried out using a commercial software, ANSYS Fluent version 2021 R1. A combination of sub models consisting of turbulence, heat transfer, fuel combustion, and gaseous transport are used in the model. The most appropriate model for swirling flows in terms of stability, and result dependability is SST k-w turbulence model, used to enclose the time-averaged conservation equations for mass and momentum. The gas phase is described as Eulerian and alumina particles are considered as Lagrangian. The flow-field of solids, and interaction with gas is defined using the two-way coupled approach of Discrete phase model (DPM). By integrating the force balance on the particle, the trajectory of the particles is computed. The particles are distributed in a size range of 20 to 150 µm. With a spread parameter of 3.5 and groups of 5, the Rosin Rammler distribution is assumed to govern the particle size of alumina hydrate.

For solving combustion, DPM is used to describe the trajectory of droplets. The fuel properties and subsequent volumetric reactions are defined using species transport model. The model allows the evaporation and burning of hydrocarbon along with the formation of non-volatile components. The P1 model is used to solve the radiation transfer equation [9]. The relevant computational equations can be referred from the literature [10]. The simulation is performed only for the furnace and separating cyclone of the calciner circuit as shown in Figure 2. The furnace is connected to the cyclone which separates the gas and solid particles. The grid for the computational domain is constructed using 1.5 million polyhedral cells and are refined at regions with high flow gradients.

Defining appropriate boundary condition is critical to understand the actual behaviour of the domain. The gas flow entering the bottom inlet is defined as mass flow with measured temperature. At the walls, no-slip boundary condition is prescribed. Actual refractory thickness is defined along with the thermal conductivity. The heat transfer coefficient of air i.e. 10 $W/m^2{\cdot}K$ is defined with ambient temperature of 30 °C.

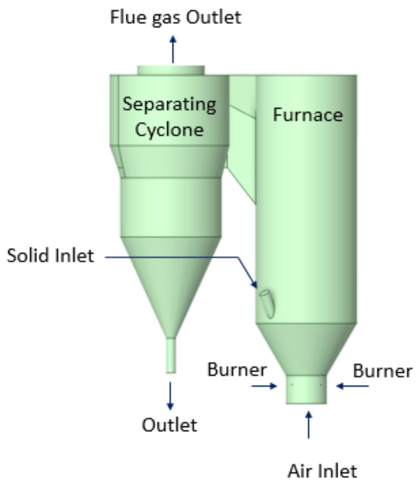

Figure 2. Schematic of furnace and separating cyclone.

3. Results and Discussion

3.1 Characterization of Calcined Alumina

To determine the quality of calcined alumina, the specific surface area and LOI are analysed at generally operated furnace temperature of 1150 °C, and the results are shown in Table 1. The specific surface area and LOI are temperature dependent quality parameters. The results show that the surface area and LOI are lower, compared to the usual requirement of smelting grade i.e. 70–80 m^2/g and 0.8 wt.% to 1.0 wt.%, respectively. To investigate the reason, the phase composition of alumina is determined using XRD analysis and is presented in Figure 3.

Table 1. BET surface area and LOI analysis.

Analysis	BET Surface Area (m^2/g)	LOI (%)
Value	53	0.4

Table 2. Quantification of alumina phases through Rietveld analysis.

Phase	Rexp	Rwp	GOF	Gamma	Delta	Theta	Alpha
GSC @1150 °C	2.31	11.82	5.1	56.3	2.6	34.5	6.5

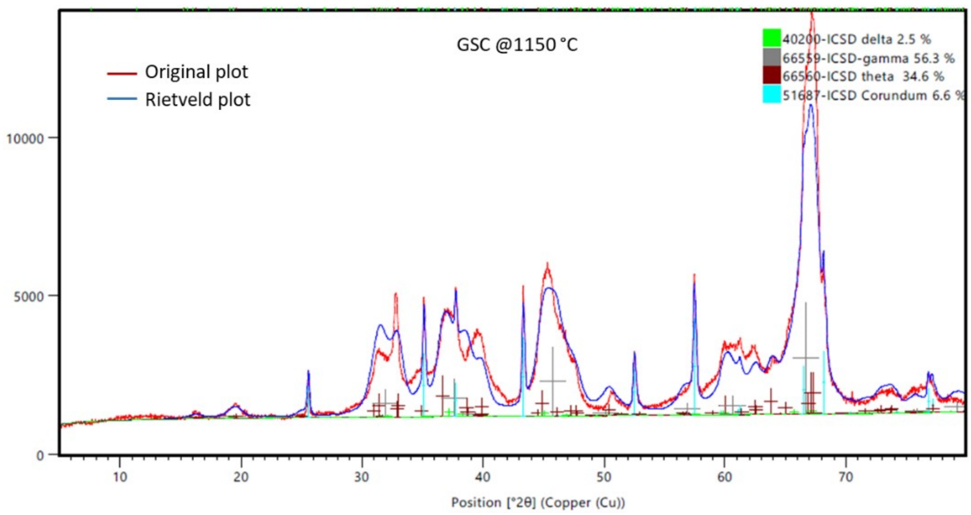

Figure 3. XRD analysis of calcined alumina sample.

The XRD pattern of the base case calcined alumina sample detected large peaks for theta and alpha along with the gamma phase. The delta phase of alumina has a similar diffraction pattern as gamma, hence a close similarity in the structure of gamma and delta phase can be assumed [11]. The mineralogical compositions of the alumina samples estimated by XRD analysis along with figure of merits are summarized in Table 2. The estimation is made by Rietveld refinement of randomly oriented samples using the known mineralogy of the alumina. It should be noted that the phase quantification shows a general trend, and therefore to be considered as semi-quantitative values. The goodness of fit (GoF) value can be improved by further inclusion of transition alumina [12]. However, the precision of Rietveld analysis becomes lower when this transition alumina coexists with low crystallinity components.

The formation of alpha and particularly theta in the higher quantities reveal the reason behind the lower values of specific surface area and LOI. With the furnace being exposed to higher temperature, the alumina is highly calcined leading to the formation of monoclinic theta and hexagonal alpha crystal structures. Furthermore, at high temperature exposure, theta alumina transforms into corundum (alpha) and significant grain growth occurs [13]. The pore structure of alumina collapses; hence, as it transforms from theta to alpha, the surface area gradually decreases. It is reported that the dissolution time decreases with increase in surface area as dissolution of alumina in electrolyte bath is a mass transfer-controlled step [14]. Hence, it is recommended to maintain the surface area from 70–80 m^2/g to achieve better dissolution of alumina [15]. The density of gamma, theta and alpha are 3.0, 3.37, and 3.98 g/cm^3 respectively [16]. As the bath density is close to 2.1 g/cm^3 [17], there is a higher probability of theta and alpha settling faster than gamma alumina. Hence, it is recommended to increase the lower order transition alumina (i.e. gamma and delta) in the final calcined alumina to improve dispersion in the bath promoting dissolution and reducing the risk of local anode effects.

3.2 CFD simulation of GSC calciner

The GSC calciner considered in the present study is operated between 60 to 70 tonnes per hour (TPH) of alumina hydrate feed rate. The air flow rate is regulated by controlling the speed of the Induced Draft fan. The fuel flow rate is adjusted as per the temperature requirement. To get a fair understanding of the process the air to fuel ratio is calculated and is typically observed to be between 21 to 28. The details about the operating parameters are shown in Table 3. The gas suspension calciner is usually operated in fast fluidization regime where higher heat transfer rate between gas and solid are achieved. Hence, the A/F ratio is maintained above the theoretical requirement of LSHS combustion i.e. 14. The gas-solid interaction plays a major role on the flow pattern inside the furnace. Since the alumina hydrate particle has a wide range of particle size distribution, there will be significant influence of gas velocities on fine and coarse fraction of particles. This may cause maldistribution of flow resulting in varying solid residence time when the calciner operated with a broad A/F ratio. It is important to understand the internal flow pattern as well as temperature profile within the calciner. They will impact the solid phase transformations in the calciner. CFD is a useful technique for examining the multiphase flow inside the calciner. The insights provided regarding flow and thermal patterns aid in understanding the calciner's performance at different operating circumstances.

Table 3. Operating parameters of GSC calciner.

Feed Rate (TPH)	Air Flowrate (kg/h)	Fuel Flowrate (kg/h)	Air to Fuel ratio
60–70	65 000–95 000	2 600–3 200	21–28

For brevity, in this paper the CFD studies for 70 TPH is discussed in detail. The velocity magnitude profile is shown in Figure 4(a), where high velocity regions can be observed in the cyclone. The volume averaged velocity in the furnace is 10.5 m/s. The trajectory of particle with respect to the residence time is shown in Figure 4(b). Validating the numerical model that is being utilized requires comparing numerical results with actual measurements. Two temperature readings from the calciner are used to compare the numerical predictions. Each of the temperature indicators are located the top of furnace and separating cyclone. The temperature field for the case simulated for the hydrate feed rate of 70 TPH is shown in Figure 4(c). The case is simulated for an air to fuel ratio of 24. It can be observed that, more regions of high temperature are observed in the furnace. The heat released by the fuel is utilized by hydrate particles for calcination. A slightly lower temperature is observed in the separating cyclone. The comparison between the actual measured results and the CFD predicted values are listed in Table 4. Although the predicted values are slightly higher, the results are in good agreement (error less than 2.5 %) with the measured data.

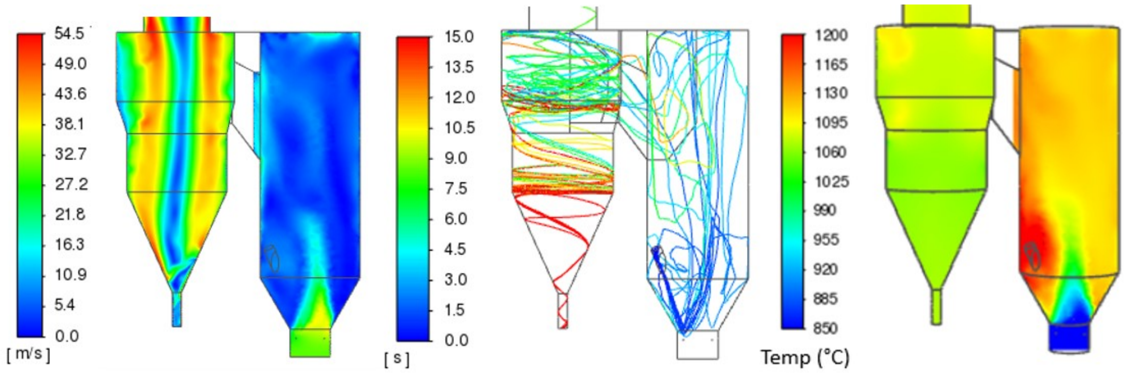

(a) (b) (c)

Figure 4. Contours for 70 TPH alumina hydrate flowrate (a) velocity magnitude (b) particle residence time (c) temperature profile.

With the understanding gained from phase analysis, the temperature of the furnace needs to be reduced to avoid over calcination and ensure uniform temperature profile. Hence, simulations are conducted at different air to fuel ratios (A/F) for reduced fuel flow rate with a target temperature of 1050 °C in the furnace [8]. The CFD study is performed for 70 TPH of hydrate feed rate and results are shown in Fig. 5. In case of A/F ~ 21, as shown in Figure 5(a), it can be observed that the residence time of hot gases increases due to lower air flow rate. Hence, high temperature regions are observed in the furnace as well as separating cyclone. Similar observation can be made from Figure 5(d), for A/F ~ 21 higher particle residence time is observed with tendency of particle movement towards the cyclone due to the influence of draft. In the case of A/F ~ 28, as shown in Figure 5(c) and 5(f), due to higher gas velocity, flow channelling is observed along with lower particle residence time. Hence, cold spots are found in the core of the furnace. Both in the case of higher and lower values of A/F ratio, a flow biasness is observed. For A/F ~ 23, a high temperature region is found only in the combustion zone of the furnace and the flow is more uniform as shown in Figure 5(b). Uniform distribution of particles can also be observed for A/F ~ 23 as shown in Figure 5(e). The temperature attained at the top of the furnace for different A/F ratios is shown in Table 5. It can be observed that along with thermal uniformity, the target temperature of 1050 °C is obtained when A/F ratio ~ 23. The simulations are also performed for 60 TPH, where similar to 70 TPH, uniform flow and thermal profile is observed for A/F ~ 23.

Maintaining uniform temperature distribution is important for the alumina phase composition of the final product alumina. Although gas suspension calciners have shorter residence time, the temperature gradients may induce inhomogeneity of the final phases being formed, hence uniform thermal profiles are necessary in calciner operation.

Table 4. Comparison of actual and CFD predicted temperature.

Location	Furnace	Cyclone
Actual temp (°C)	1129	1062
CFD temp (°C)	1105	1040

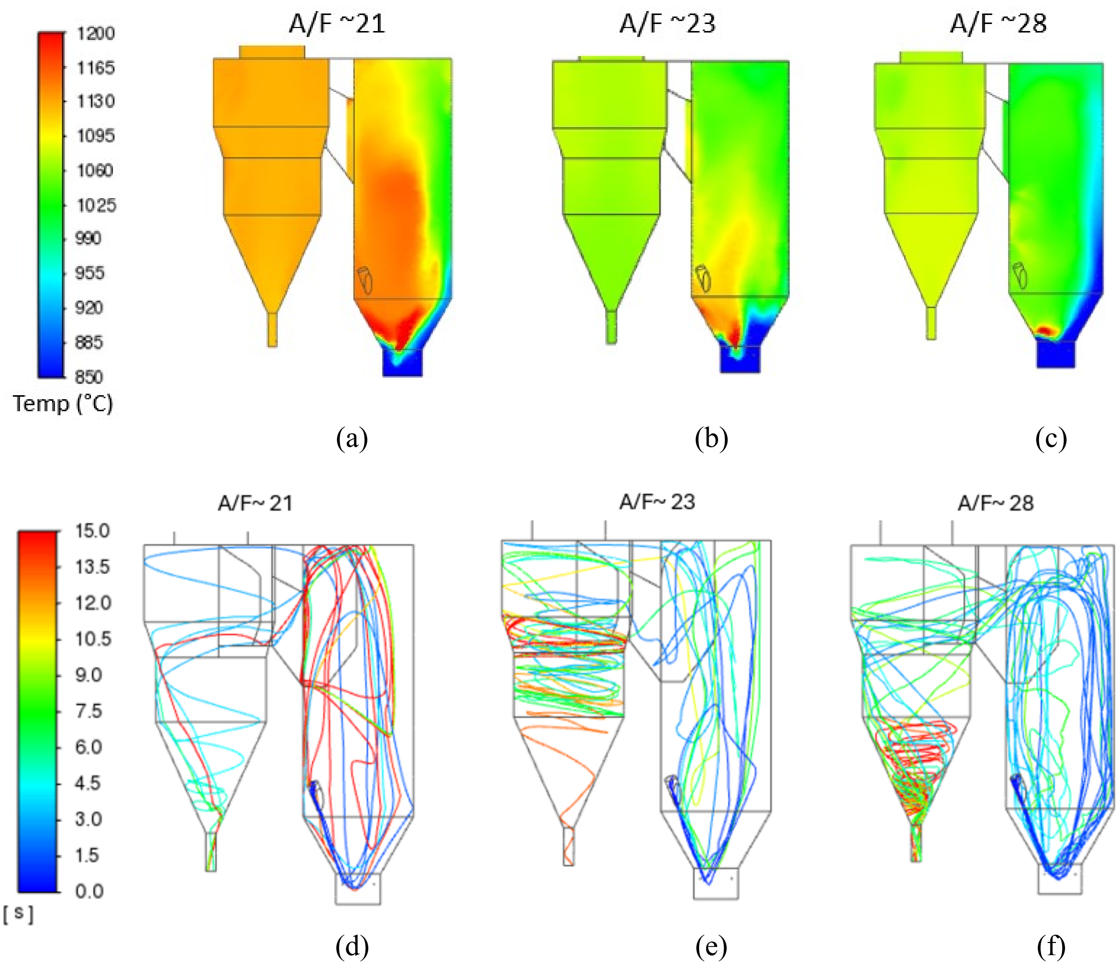

Figure 5. Contour for 70 TPH alumina hydrate flowrate with varying A/F ratio (a to c) temperature profile, (d to f) particle residence time.

Table 5. CFD predicted furnace temperature for various A/F ratio.

A/F	21	23	28
Temperature (°C)	1108	1055	1010

3.3 Onsite Trials

Onsite trials are conducted with an objective to obtain alumina with a higher amount of gamma content. Hence, the furnace temperature is reduced along with the optimized flow profile at suggested A/F~23 by maintaining the induced draft fan between 510 to 515 rotation per minute (RPM). During the study, the hydrate feed rate is maintained constant at around 65 TPH, as per the production requirement at the moment. The furnace temperature is gradually reduced by lowering the fuel flowrate as shown in Figure 6(a). The specific surface area of the calcined alumina is measured at regular intervals to monitor the quality. As shown in Figure 6(b), the surface area of the calcined alumina increased with the lowering the furnace temperature. The temperature is reduced till SSA reached between 70–80 m^2/g and LOI is close 0.7 wt.%. Overall, the temperature is reduced from 1140 °C to 1075 °C due to constraints of lower stack temperature. Typically, LSHS fuel contains 0.5–1 % Sulphur with acid dew point in the range of 120–130 °C [18]. Hence, the stack temperature is maintained 10ºC above the acid dew point to avoid corrosion in ESP and stack.

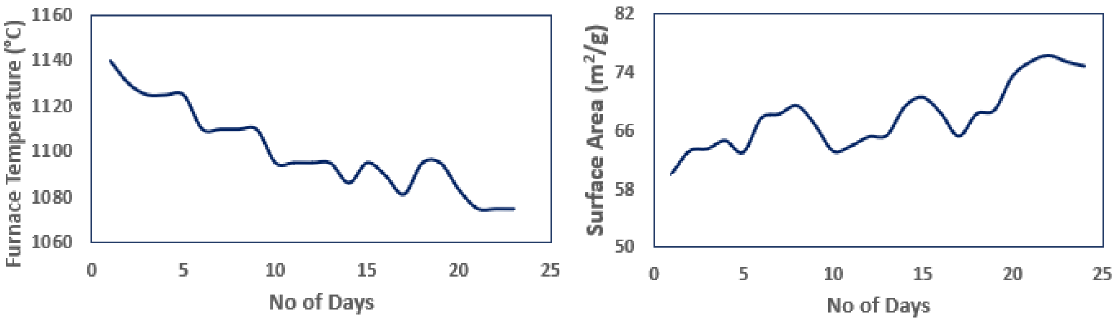

(a) (b)

Figure 6. Onsite trial results (a) Furnace temperature, (b) BET surface area.

The XRD phase analysis of the final calcined alumina is performed to determine the quality of alumina. The overlay of XRD graphs between the base case and final sample at optimized conditions is shown in Figure 7. The Rietveld refinement for final calcined sample is performed to quantify phases (R_{exp} =2.27, R_{wp} = 11.8 and GOF = 5.2). From Table 6, it can be observed that, there is an increase in delta alumina content from 2.6 wt.% to 36.2 wt.%, and the intermediate theta phase is reduced significantly to < 1 %. The alpha phase also reduced from 6 wt.% to 3 wt.%. This indicates that the over calcination of alumina is minimized. Along with temperature reduction, maintaining A/F ratio of 23 has helped in reducing theta and alpha formation due to exposure of particles to extreme temperature conditions. The particle size distribution of calcined alumina is also measured and monitored after reducing the calciner temperature. The percentage fine generation (< 45 µm) remained same and varied in the range of 8 to 10 wt%.

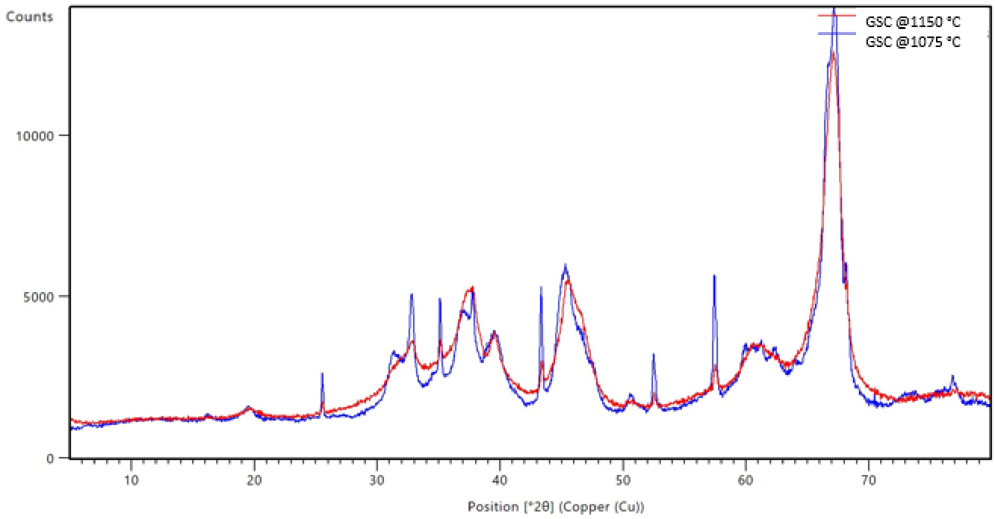

Figure 7. Comparison of XRD patterns for calcined alumina at two different furnace temperature (a) red line – GSC at 1150 °C and (b) blue line – GSC at 1075 °C.

Table 6. Comparison alumina phase quantification.

Phase	GSC @1150 °C Content (%)	GSC @1075 °C Content (%)
Gamma	56.3	60.8
Delta	2.6	36.2
Theta	34.5	<1
Alpha	6.5	3

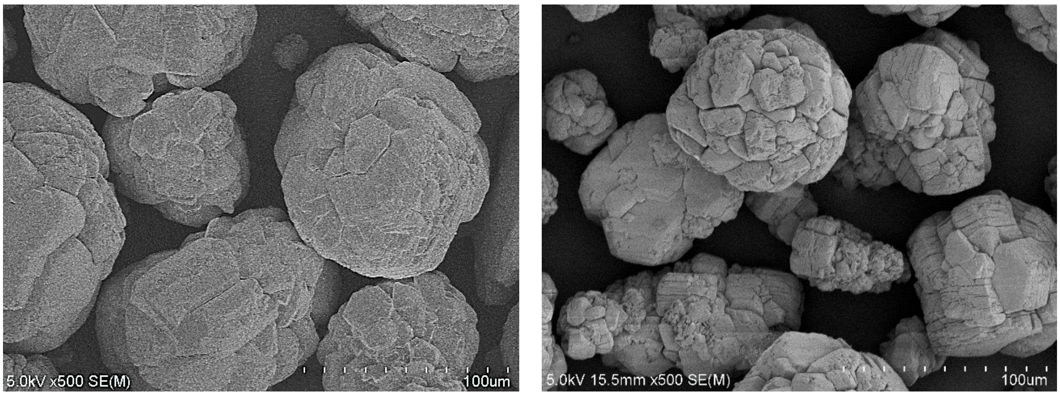

(a) (b)

Figure 8. SEM images of calcined alumina for two different furnace temperature (a) GSC at 1150 °C and (b) GSC at 1075 °C.

To analyse the morphology of the calcined alumina, SEM analyses are conducted. The SEM images of particles calcined at two different temperatures are shown in Figure 8. Although, it is difficult to distinguish any morphological changes for such a small temperature gradient, at high temperature it can be observed that the crystallite grains are rigidly bound to each other due to sintering effects. However, as shown in Figure 8(b), the fragments of crystallite particles are observed with internal defects. This qualitative analysis is complimented by higher surface area observation from BET analysis. Since, dissolution of alumina in electrolyte bath is a phenomenon controlled by diffusion, alumina with higher surface area accelerates the rate of dissolution.

By bringing the calciner in the new regime of lower temperature operation, the overall specific fuel energy requirement for producing calcined alumina is reduced. With a reduction of furnace top temperature from 1140 °C to 1075 °C, the specific fuel consumption has reduced by 0.66 kg/t. By streamlining the A/F ratio ~ 23, more uniform flow and thermal profile is achieved. This minimizes thermal energy being lost in raising the temperature of preheated air entering the furnace from cooling cyclone in case of high A/F ratio. The temperature reduction has also favoured intangible benefits such as reduction in the radiational losses and better durability of the refractory lining.

4. Conclusions

The aim of the present work is to achieve the quality of alumina as per the smelter requirements. The study is performed by characterizing the alumina using techniques such as XRD, SEM and BET surface area. The characterization showed an over-calcined product with lower specific surface area and LOI than the desired values for smelting. A set of CFD simulation studies were performed to provide optimal operating conditions by reducing the draft and maintaining air to fuel ratio at approximately 23. The temperature of the furnace is reduced to 1075 °C such that the properties of alumina could facilitate desired requirements for efficient performance in the smelter. Onsite trials supported the findings and resulted in reduction of specific fuel consumption by 0.66 kg/t.

5. Acknowledgements

The authors would like to thank the management of Hindalco Industries Ltd, Renukoot and ABSTC for their continuous support and guidance during the execution of the research work. Special thanks to Analytical Science and Technology Department of ABSTC for their support in characterization. Authors would like to express their gratitude to Mrs. Pranjali Joshi (ABSTC) for her extensive support in XRD analysis.

6. Reference

1. Habashi. Fathi, "A hundred years of the Bayer process for alumina production." *In Essential Readings in Light Metals: Volume 1 Alumina and Bauxite*, pp. 85-93, Cham: Springer International Publishing, 2016.
2. Gerlach, J., Hennig, U. and Kern, K. “The dissolution of aluminum oxide in cryolite melts”, *Metallurgical and Materials Transactions B*, 6, pp.83-86, 1975.
3. A.Boumaza, L.Favaro, J.Ledion, G.Sattonnay, J.B.Brubach, P.Berthet, A.M.Huntz, P.Roy, R.Tetot, “Transition alumina phases induced by heat treatment of boehmite: An X-ray diffraction and infrared spectroscopy study”, *Journal of Solid State Chemistry*, 182, 1171–1176, 2009.
4. Perander, Linus M., James B. Metson, and Cornelis Klett. "Two perspectives on the evolution and future of alumina", *TMS Light Metals 2011*, edited by Stephen J. Lindsay, pp. 151-155.
5. Fallah Fini, M., Landry, J. R., Soucy, G., Désilets, M., Pelletier, P., Rivoaland, L., & Lombard, D. “Sludge Formation in Hall–Héroult Cells: Drawbacks and Significant Parameters”, *Mineral Processing and Extractive Metallurgy Review*, 41(1), 59–74, 2020.
6. Anich, Ivan, Tony Bagshaw, Nancy Margolis, and Mike Skillingberg. "The alumina technology roadmap." *In Essential Readings in Light Metals: Volume 1 Alumina and Bauxite*, pp. 94-99. Cham: Springer International Publishing, 2016.
7. Perander, L.M., Zujovic, Z.D., Kemp, T.F. et al. “The nature and impacts of fines in smelter-grade alumina”, *JOM* 61, 33–39, 2009
8. Jaganathan, Pungkuntran & Pragasam, Senthilkumar “Experience Driven Design Improvements of Gas Suspension Calciners” *TRAVAUX 48, Proceedings of the 37th International ICSOBA Conference*, Krasnoyarsk, Russia, 2019
9. Mao, Ya, Di Zhang, Zuobing Chen, Zhi Jiang, Xiang Chen, and Yuhua Deng. "Numerical modelling of multiphase FLOW and calcination process in an industrial calciner with fuel of heavy oil". *Powder technology*, 363, 387-397, 2020.
10. A. Fluent, ANSYS Fluent Theory Guide, http://www.ansys.com. 2022
11. Jiménez, Jose A., Isabel Padilla, Aurora López-Delgado, Laila Fillali, and Sol López-Andrés. "Characterization of the aluminas formed during the thermal decomposition of boehmite by the Rietveld refinement method", *International Journal of Applied Ceramic Technology*, 12, 178-186, 2015.
12. Metson, James, Tania Groutso, Margaret Hyland, and Scott Powell. "Evolution of microstructure and properties of SGA with calcination of Bayer gibbsite", *TMS Light Metals 2006,* edited by Travis J. Galloway, pp.89-93.
13. Levin, I. and D. Brandon “Metastable alumina polymorphs: crystal structures and transition sequences”, *Journal of the American Ceramic Society*, 81(8): p. 1995-2012, 1998.
14. Yang, Youjian, Bingliang Gao, Zhaowen Wang, Zhongning Shi, and Xianwei Hu. "Effect of physiochemical properties and bath chemistry on alumina dissolution rate in cryolite

electrolyte", *The Journal of The Minerals, Metals & Materials Society*, 67, 973-983, 2015.

15. Benny E. Raahauge, Fred S. Williams "Smelter Grade Alumina from Bauxite: History, Best Practices, and Future Challenges", Springer Series in Material Science, 2022
16. Zamorategui, Adrian, Satoshi Sugita, Ramon Zarraga, Satoshi Tanaka, and Keizo Uematsu. "Evaluation of dispersability of gamma alumina prepared by homogeneous precipitation", *Journal of the Ceramic Society of Japan* 120, no. 1403, 290-294, 2012.
17. Cassayre, Laurent, Patrice Palau, Pierre Chamelot, and Laurent Massot. "Properties of low temperature melting electrolytes for the aluminum electrolysis process: a review", *Journal of Chemical & Engineering Data* 55, no. 11, 4549-4560, 2010.
18. ZareNezhad, B. "A General Correlation for Accurate Prediction of the Dew Points of Acidic Combustion Gases in Petroleum Industry", *Petroleum science and technology* 32, no. 16, 1988-1995, 2014.